

## Incorporating environmental variability in a spatially-explicit individual-based model of European sea bass<sup>☆</sup>

Joseph W Watson<sup>a,d,\*</sup>, Robin Boyd<sup>b</sup>, Ritabrata Dutta<sup>c</sup>, Georgios Vasdekis<sup>c</sup>, Nicola D. Walker<sup>d</sup>, Shovonlal Roy<sup>e</sup>, Richard Everitt<sup>c</sup>, Kieran Hyder<sup>d,f</sup>, Richard M Sibly<sup>a</sup>

<sup>a</sup> School of Biological Sciences, University of Reading, Whiteknights, Reading RG6 6AB, UK

<sup>b</sup> UK Centre for Ecology and Hydrology, Wallingford, UK

<sup>c</sup> Department of Statistics, University of Warwick, UK

<sup>d</sup> Centre for Environment, Fisheries & Aquaculture Science, Lowestoft Laboratory, Pakefield Road, Lowestoft NR33 0HT, UK

<sup>e</sup> Department of Geography and Environmental Science, University of Reading, Whiteknights, Reading RG6 6AB, UK

<sup>f</sup> School of Environmental Sciences, University of East Anglia, Norwich Research Park, Norwich, Norfolk NR4 7TJ, UK

### ARTICLE INFO

#### Keywords:

Individual based modelling  
Agent based modelling  
European sea bass  
*Dicentrarchus labrax*  
Fisheries management  
Approximate Bayesian Computation

### ABSTRACT

The northern stock of European sea bass (*Dicentrarchus labrax*) is a large, high value, slow growing and late maturing fish that is an important target species for both commercial and recreational fisheries. Around the UK, scientific assessments have shown a rapid eight-year decline in spawning stock biomass since 2010 attributed to poor recruitment; this was likely driven by environmental factors and high fishing mortality. Management of the stock is informed by scientific assessments in which a population model is fitted to the available data and used to forecast the possible consequences of various catch options. However, the model currently used cannot represent the spatial distribution of the stock or any effects of environmental variability. One approach that may be used to represent the effects of spatial and temporal variation in environmental drivers is with Individual based models (IBMs). In IBMs populations are represented by their constituent individuals that interact with their environment and each other. The mechanistic nature of IBMs is often advantageous as a management tool for complex systems including fisheries. Here we add to an existing IBM to produce a spatio-temporally explicit IBM of the northern stock of sea bass in which individual fish respond to local food supply and sea surface temperature. All life stages (i.e., pelagic stages, juvenile and mature fish) are modelled and individual fish have their own realistic energy budgets driven by observed dynamic maps of phytoplankton density and sea surface temperature. The model is calibrated using Approximate Bayesian Computation (ABC). After calibration by ABC the model gives good fits to key population parameters including spawning stock biomass. The model provides a mechanistic link between observed local food supplies and sea surface temperatures and overall population dynamics. Plots of spatial biomass distribution show how the model uses the energy budget to predict spatial and temporal change in sea bass biomass distribution in response to environmental variability. Our results indicate that the IBM is a promising approach that could be used to support stock assessment with scope for testing a range of spatially and temporally explicit management scenarios in addition to testing stock responses to novel environmental change.

### 1. Introduction

The European sea bass (*Dicentrarchus labrax*) has been an important target species for commercial and recreational fishers around the UK for more than 50 years, however after decades of exploitation and minimal

regulation the stock began to rapidly decline in 2010 (Pickett and Pawson, 1994; ICES, 2021). The decline continued for eight years and was attributed to a combination of poor recruitment and fishing mortality which led to the implementation of emergency management measures in 2015 with continuing stringent harvest restrictions to

<sup>☆</sup>Joseph W Watson, Robin Boyd, Ritabrata Dutta, Georgios Vasdekis, Nicola Walker, Shovonlal Roy, Richard Everitt, Kieran Hyder, and Richard Sibly made contributions as authors. JW led the writing of the manuscript. All authors contributed to model development and gave critical comments on each draft of the manuscript. All authors gave permission for submission having seen the final draft.

\* Corresponding author.

E-mail address: [joseph.watson@cefas.co.uk](mailto:joseph.watson@cefas.co.uk) (J.W. Watson).

<https://doi.org/10.1016/j.ecolmodel.2022.109878>

Received 28 July 2021; Received in revised form 22 December 2021; Accepted 11 January 2022

Available online 21 January 2022

0304-3800/© 2022 The Authors.

Published by Elsevier B.V. This is an open access article under the CC BY-NC-ND license

(<http://creativecommons.org/licenses/by-nc-nd/4.0/>).

present day (ICES, 2019, 2021). Sea bass are a slow growing, long lived, generalist predator with a complex life cycle that includes feeding and spawning migrations (Pickett and Pawson, 1994). A further complex component of the sea bass life cycle is the recruitment process (i.e., the surviving from egg through larval stages to a harvestable fish) which is particularly precarious and influenced by many drivers, the result of which can be observed as recruitment rates with high levels of inter-annual variation (Pickett and Pawson, 1994; ICES, 2021). These life history components make the building of assessment models for this stock particularly challenging.

The northern sea bass stock is assessed by the International Council for the Exploration of the Sea (ICES) using Stock Synthesis 3 (SS3); an analytical age- and length-based assessment model optimized for tactical management (ICES, 2019). SS3 includes: 1) a population dynamics model, which represents growth, mortality, and recruitment; 2) an observation model which relates the population dynamics to available data; and 3) a statistical model which estimates parameters to maximise the goodness of fit between population model and data. While SS3 is well-suited for use in tactical management, there are important strategic questions which it cannot, and is not designed, to answer. First, SS3 can include only a crude representation of the spatial distribution of the stock using its “multi-area” configuration (Methot and Wetzel, 2013). For this reason it is limited in its ability to represent the effects of spatial management scenarios (e.g., sea bass fishery spatial closures in key spawning areas [GOV.UK, 2020]). Second, SS3 does not represent the effects of environmental variability on the stock; for this reason it cannot make predictions about how the stock will develop against uncertain climate backdrops, or how climate uncertainty might interact with harvesting scenarios e.g., Boyd, Thorpe, et al., 2020.

Walker et al. (2020) developed an individual-based model for European sea bass. This model and others like it are widely used to simulate the spatial distribution of fish populations (Watkins and Rose, 2017; Heinänen et al., 2018; Boyd, Walker, et al., 2020), as well as population size and structure (Politikos, Huret and Petitgas, 2015; Boyd, Walker, et al., 2020; Bueno-Pardo et al., 2020). In Walker et al. (2020) the stock's spatial distribution results from algorithms that govern the movements of the individuals, but the population dynamics component is that of SS3. The logical next step is to allow individual vital rates to respond to observed local variation in key environmental drivers. To do so one must first identify important environmental drivers, and then incorporate sub-models that describe the ways in which individuals respond to these drivers.

Prey availability and temperature are two key environmental drivers that affect rates of growth and reproduction in sea bass and ultimately population dynamics (Pickett and Pawson, 1994). The effects of prey availability and temperature on fish are typically modelled using energy budgets (sometimes called bioenergetics). Our energy budget approach follows an established methodology (Sibly et al., 2013) that has been used for a range of species and applications (Sibly et al., 2013; Grimm et al., 2014; van der Vaart et al., 2015; Boulton et al., 2019; Boyd, Walker, et al., 2020; Mintram et al., 2020; Watson et al., 2020). The energy budget models describe the acquisition of energy from food in the environment and its allocation to maintenance (metabolism), growth, reproduction, and energy storage. Rates of acquisition and expenditure depend on temperature and body size, and these can be modelled using established theoretical relationships. Recently, bioenergetics models have been implemented in IBMs which enables extrapolation of the individual-level effects of prey availability and temperature (e.g., on body size and reproductive output) to the population level (Boyd, Walker, et al., 2020). Here we use phytoplankton density and sea surface temperature (SST), assessed through remote sensing. Phytoplankton density is used as an index of food supply and together with SST drives the energy budgets of individual fish. The energy budgets link population dynamics to environmental drivers and ultimately outputs the population metrics that are used in fisheries management.

In this study, we extend the model of Walker et al. (2020)

incorporating a bioenergetics module to account for spatio-temporal variation in prey availability and temperature. Information on prey availability and temperature are derived from two satellite products: chlorophyll concentration, which we use as a proxy for prey availability (this is discussed further in the Discussion); and sea surface temperature (SST). We estimate five parameters of the bioenergetics model by fitting the IBM to individual- and population-level outputs from the latest stock assessment. We show that the calibrated model matches the stock assessment outputs well, and we show some spatial outputs to demonstrate how the model links environmental drivers to spatial and temporal distribution of sea bass biomass. Finally, we discuss the potential utility of our model for strategic management of the European sea bass stock.

## 2. Methods

### 2.1. Overview

Here we provide a summary description of the IBM. A full description following the ODD (Overview, Design concepts, Details) protocol for describing individual- and agent based models (Grimm et al., 2006, 2010, 2020) is provided in a TRACE (TRANSPARENT and Comprehensive model Evaluation; Augusiak, Van den Brink, & Grimm, 2014; DeAngelis & Grimm, 2014; Schmolke, Thorbek, DeAngelis, & Grimm, 2010) document forming the supplementary material. The IBM is implemented in Netlogo version 5.3.1 (Wilensky, 1999). The code and dataset used for this research, can be downloaded from <https://github.com/eth-cscs/abc-py-models/tree/master/EcologicalScience/Bass>. The model develops the approach of Walker et al. (2020) to include energy budgets for individual fish. The model environment is composed of a grid landscape of  $36 \times 38$  patches (grid cells), representing the area from  $9^\circ\text{E}$  to  $9^\circ\text{W}$  and  $48^\circ\text{N}$  to  $57.5^\circ\text{N}$  (Fig. 1). The model uses dynamic patch variables of sea surface temperature (SST [shown in blue Fig. 1A]; a key driver of sea bass dynamics; Pickett & Pawson, 1994; TRACE Section 8.2 and 10.2). SST in the model affects all life processes including ingestion rate, maintenance (i.e., metabolic rate), growth (note that this means SST also effects the speed at which individuals reach the next life stage), swimming speed and spawning (i.e., reproduction). The model now also includes a patch variable of phytoplankton density (PHY [shown in orange Fig. 1B], derived from chlorophyll concentration using an empirical conversion factor; see Discussion and TRACE Sections 8.2 and 10.3 for discussion of the role of PHY as a base of the marine food web and the basis for energy in our energy budget update. The patches of the model environment are categorised depending on location within the environment (Fig. 1). Coastal patches are those within an ICES rectangle (ICES rectangles/divisions are a fisheries management system that grids data for ease of spatial analysis and management measures, for more details see ICES statistical rectangles) that intersects land and offshore patches are all remaining sea patches. Between February–May any offshore patches south of  $54^\circ\text{N}$  with an SST value between  $9\text{--}15^\circ\text{C}$  are assigned as spawning patches (Thompson and Harrop, 1987; Kelley, 1988; Beraud et al., 2018). Nursery patches are those south of  $54^\circ\text{N}$  intersecting land; (Kelley, 1988; Beraud et al., 2018). Patches are also assigned an ICES division (each of which comprises many ICES rectangles; 4.b, 4.c, 7.a, 7.d, 7.e or 7.f.g) and region (North Sea, English Channel, Celtic Sea or Irish Sea). ICES divisions and regions are mutually exclusive while patch types are not, as all nursery patches are coastal, and all spawning patches are offshore (Fig. 1).

For simplicity, we assume the population is closed to migration outside the model domain. To keep model run times practical the sea bass population is modelled with super-individuals (hereafter termed individuals) each of which represents many fish with identical state variables (Scheffer et al., 1995). Individuals are characterised by; the number of fish represented, age, life stage (see Figs. 1 and 2 and sub model *Transform*), length, weight (including structural mass, gonad mass and total mass), ingested energy, energy reserves, metabolic rate,

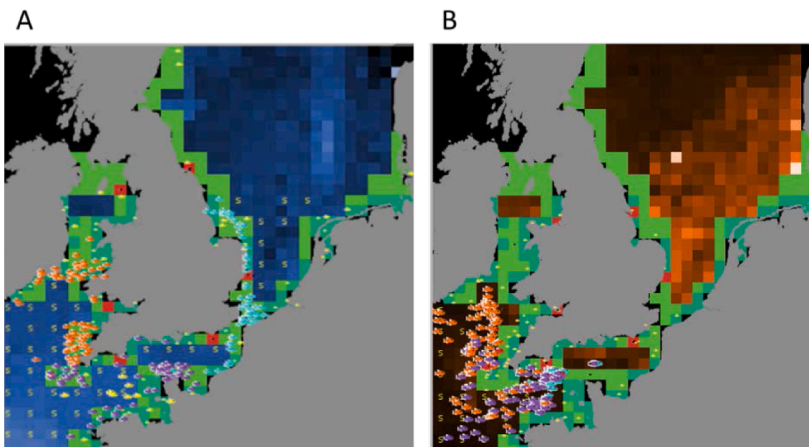


**Fig. 1.** The model interface; Both Sea surface temperature (SST) and phytoplankton concentration (PHY) can not be shown simultaneously in the model interface so here; A) shows offshore patches as blue with dark to light representing increasing SST (min and max potential values 0–30 °C), and B) shows offshore patches as orange with dark to light representing increasing PHY (min and max potential values 0–75 g/m<sup>2</sup>). For both A) and B) coastal patches represented in green, nursery patches (also coastal) are turquoise. Targets that eggs and larval stages drift towards (depending on ICES division affinity) are represented by red patches. Agent colour represents life stage (white = eggs, black = yolk sacs-larvae and larvae, yellow = juvenile sea bass [not all life stages are shown here]). For mature sea bass colour shows the affinity to feeding ground. Spawning patches (which vary depending on time of year and environmental conditions) are shown with a yellow ‘S’. These remote sensing data are updated every 8 days and agents perform all sub models each day (see section below 2.1.2).

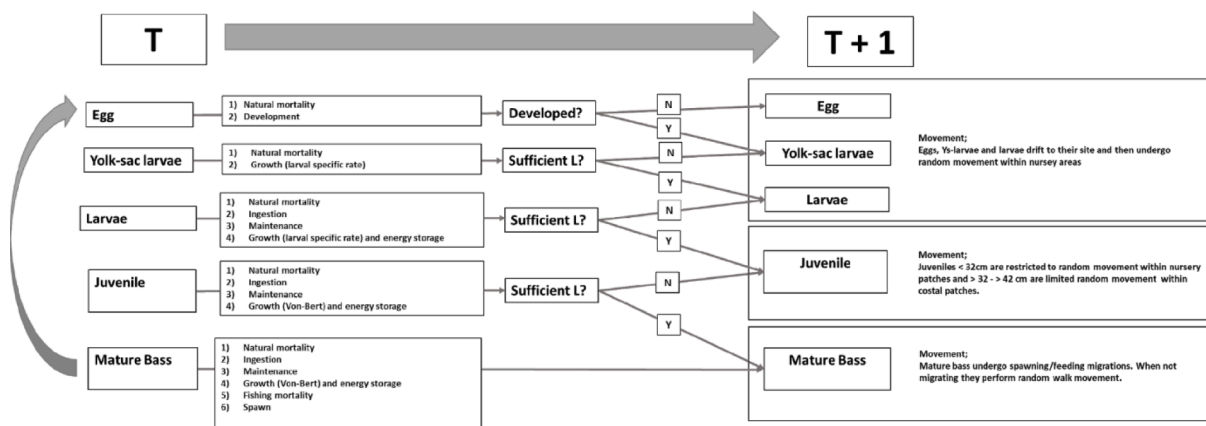


**Fig. 2.** Model overview showing for each life stage the processes occurring on day T. Transformation to the next life stage at the end of the day is a length-based process and “sufficient L” refers to a specified body length being reached to transform. For each life stage (egg, yolk-sac larvae, larvae, juvenile, and mature sea bass) the sub models are indicated in the order of model execution. Eggs transform to the next life stage after a specified time and from then on transformation is length based. Overviews of movement sub models are given on the right (for more details see TRACE section 7).

location, swimming speed and daily direction changes, spawning trigger and counter, mortality rates (natural, commercial inshore/offshore fishing mortality and recreational-fishing mortality) and the division they have an affinity to feed in. Sea bass variables and processes are described further in Section 2.1.2 and full details can be found in the TRACE. After an initial spin up (1985–2004), the model runs in daily time steps from 1st of January 2004 to the 31st of December 2014, just prior to the implementation of emergency management measures in 2015 (ICES, 2021). In each time step, individuals follow six main processes, all constructed from several sub models: *ingestion and assimilation*, *maintenance* (i.e., *metabolic rate*) and *reserves*, *growth*, reproduction (i.e., *spawning*), movement, and mortality. Fig. 2 provides a conceptual overview of the processes and sub models relevant to the different life stages represented in the IBM. In the following sections we give an overview of these sub models, highlighting the new energy budget updates and directing the reader towards relevant supplementary materials (TRACE sections) for further details.

2.1.1. Initialization and spin up

The model is initialised on 1st of January 1985 and runs with daily

time steps for a 19-year spin-up period. Thereafter emergent results are collected from 1st of January 2004 until 31st of December 2014. During the spin up, Numbers-at-age data from the ICES stock assessment 2020 are used to base the initialized population and then each year new agents are introduced from estimates of numbers at age 0 also from the stock assessment (numbers at age 0 emerge from the simulation once the spin-up period is over). The remote sensing data for SST and PHY for 2004 is used on repeat for each year in the spin up as it was unavailable before this date (for full details of spin up see TRACE section 5).

2.1.2. Process overview and scheduling

An overview of the sub models is presented here but for complete detail we refer the reader to the relevant TRACE sections. The major addition to the model of Walker et al. (2020) are the energy budget processes and the sub models; *ingestion and assimilation*, *maintenance* (i.e., *metabolic rate*) and *reserves*, *growth* and reproduction (i.e., *spawning*). The Eqs. (1-5) that make up the energy budget approach follow an established methodology (Sibly et al., 2013) that has subsequently been used for a range of species and applications (Sibly et al., 2013; Grimm et al., 2014; van der Vaart et al., 2015; Boulton et al., 2019; Boyd, Walker,

et al., 2020; Mintram et al., 2020; Watson et al., 2020).

The model proceeds through all sub models in daily time steps. The following sub models are executed in the order they are presented. Within each sub model, super-individuals and patches are processed in a random order as there are no interactions amongst agents (an overview can be seen in Fig. 2). Agents age one day each time step and the cohort age is increased by one year every 365 time steps.

**Update-patches:** New SST and PHY data is assigned to patches, and offshore patches update their spawning patch status (though note that SST and PHY data only changes every 8 days).

**Natural mortality:** The number of fish in each super-individual is discounted by its natural mortality rate. Any super-individuals reaching the (terminal) age of 30 are removed from the simulation.

**Ingestion and assimilation:** All life stages calculate ingestion and assimilation except for eggs and egg- sac larvae as these early life stages rely on their own energy source rather than feeding (Pickett and Pawson, 1994). For the older life stages (larvae, juvenile and mature sea bass) the rates of ingestion and assimilation are dictated by size of the individual, energy available in the environment, temperature, and density dependence (i.e., intraspecific competition for food). The assimilated energy ( $E$ ) is then the energy available for the remainder of the energy budget processes (i.e., growth, maintenance, and reproduction) and is calculated as:

$$E = C_{max} * \left( \frac{PHY}{H + PHY} \right) * M_i^{\frac{2}{3}} * i * \left( \frac{1}{M_{nm}^{\frac{1}{3}}} \right) * Ep * Ae * Ah \quad (1)$$

where  $C_{max}$  is the maximum consumption of food in relation to body size,  $PHY$  is the energy value of the patch,  $H$  is the half saturation

**Table 1**  
Parameter values used in Energy budget equations.

Parameter	Description	Value	Reference
$a$	Length-mass coefficient (for details see TRACE Section 8.3).	$1.296 \times 10^{-5} * 0.95$	(Pickett and Pawson, 1994; ICES, 2012)
$b$	Length mass scaling exponent.	2.969	(ICES, 2012)
$Ao$	Normalizing constant for relationship between Metabolic rate and fish size.	0.1227808	(Claireaux, 2006; Jourdan-Pineau et al., 2010; Luna-Acosta et al., 2011; Zupa et al., 2015; Peixoto et al., 2016)
$Ae$	Efficiency of energy from phytoplankton to fish.	$1.64 \times 10^{-3}$	Parameterised with ABC
$C_{max}$	Max ingestion.	0.54 per gram of fish	(Lanari, D'Agaro and Ballestrazzi, 2002)
$E_f$	Energy content of flesh.	$7 \text{ kJ g}^{-1}$	(Peters, 1986)
$EG_m$	Sea bass egg mass.	$0.96 \times 10^{-3}$	(Cerdá et al., 1994)
$EG_{pw}$	Potential egg production per gram of sea bass.	8 375,000	(Pickett and Pawson, 1994)
$El$	Energy content of lipid.	$39.3 \text{ kJ g}^{-1}$	(Schmidt-Nielsen, 2013)
$Ep$	Energy content of phytoplankton.	$6.02 \text{ kJ g}^{-1}$	(Annis et al., 2011)
$F_s$	Energy to synthesise flesh.	$3.6 \text{ kJ g}^{-1}$	(Sibly and Calow, 1986; Sibly et al., 2013)
$GL$	Larval stages growth coefficient.	$0.02485 \text{ cm d}^{-1}$	(Jennings, Jennings and Pawson, 1992; Regner and Dulčić, 1994)
$H$	Half saturation constant	$4.87 \times 10^{-1}$	Parameterised with ABC
$I$	Importance of density on ingestion.	$5.14 \times 10^{+13}$	Parameterised with ABC
$K$	Annual growth rate coefficient.	0.096699	(ICES, 2012)
$L_{inf}$	Asymptotic length.	84.55 cm	(ICES, 2012)

constant,  $M_i$  is total mass (Note the 2/3 power refers to body surface area following Boyd et al., 2018; Kooijman & Metz, 1984),  $i$  is importance of conspecific density,  $M_{nm}$  is the sum of non-egg biomass in the same patch,  $Ep$  is the energy in phytoplankton and  $Ae$  is the product of assimilation efficiency (i.e., the proportion of energy that is absorbed from prey) and trophic delay (i.e., how long/how much energy from a phytoplankton bloom makes its way through the trophic levels to sea bass prey) and  $Ah$  is an Arrhenius function (for details see TRACE sections 7, 8.2, 10.3, and see Table 1 for parameter values).

**Maintenance and reserves:** All life stages calculate metabolic rate and its energetic cost, except for eggs and egg- sac larvae. Metabolic rate is affected by body mass and temperature, and here we calculate field metabolic rate as twice the standard metabolic rate (Peters, 1986) and is calculated as  $Mr$  below:

$$Mr = Ao * M_i^{\frac{3}{4}} * 2 * Ah \quad (2)$$

where  $Ao$  is a metabolic rate normalisation,  $M_i$  is total mass and  $Ah$  is an Arrhenius function. Once the energetic cost of maintenance/metabolic rate is established it is either paid for directly from assimilated energy or if this is insufficient (e.g., reduced feeding available in the winter) then energy reserves are added to assimilated energy and metabolic costs are taken from this (for details see TRACE sections 7 and see Table 1 for parameter values).

**Growth:** All life stages except eggs calculate their total mass (mass of an individual including, if any, fat reserves and gonad mass):

$$M_i = a * L^b + \frac{Er}{El} + Gm \quad (3)$$

where  $a$  and  $b$  are Length-mass coefficient values (for details see TRACE Section 8.3),  $Er$  is how much energy is in reserves,  $El$  is the energy content of lipid and  $Gm$  is mass of gonads.

Next the maximum possible growth increment ( $Max_{Gr}$ ) is calculated and here we assume individuals under 70 days have a constant maximum growth rate (for details see TRACE section 8.3) and those older are assumed to follow a von Bertalanffy growth curve:

$$Max_{Gr} = \begin{cases} Gl * Ah, & \text{Age} < 70 \text{ days} \\ (L_{inf} - L) * (1 - \exp(-k/365)) * Ah, & \text{Age} \geq 70 \text{ days} \end{cases} \quad (4)$$

where  $Gl$  is the slope coefficient of a regression of larval length on age,  $L_{inf}$  is the asymptotic length of sea bass,  $L$  is fish length and  $k$  is the annual growth constant and  $Ah$  is an Arrhenius function. After calculating the theoretical maximum size increase, the energetic cost of this maximum increase is calculated. Eggs do not grow, instead they develop and transform into yolk-sac larvae which do not ingest energy and thus are assumed to have maximum energy available to grow maximally. However once egg-sac larvae have transformed to larvae they begin to ingest energy and here larvae, juvenile and mature sea bass only grow maximally if there is adequate assimilated energy and update length accordingly. If there is not enough assimilated energy, they will grow at a suboptimal growth rate (for details see TRACE section 8 and see Table 1 for parameter values).

**Calculate-speed:** The swimming speed of each fish is calculated from its length and SST of the patch (for details see TRACE section 7).

**Transform:** In our model we include the full fish life cycle and use length-based definitions to distinguish between life stages. In the transform sub model if a super-individual meets the criteria (sufficient length; see Fig. 2) then it transforms to the next life stage. The life stages are egg; yolk-sac larvae; larvae; juvenile sea bass; and mature sea bass. When juveniles transition to mature sea bass, they set their coastal feeding ground affinity as the ICES division in which they are in at the time of exceeding this length requirement (this could be a different division to the original ICES division target they would have drifted towards when they were in pelagic stages, see TRACE section 8.7). Note that at the end of the first spawning migration there is an opportunity to

change ICES division affinity which is altered with a probability that can be set by the model user.

**Fishing-mortality:** For fish that are over the minimum landing sizes the number of fish represented by each super-individual is discounted by fishing mortality rates from the commercial offshore, commercial inshore and recreational fleets (data obtained from ICES stock assessment 2020).

**Movement:** Juvenile and mature movement sub models remain mostly unchanged from Walker et al., 2020. However, a major addition to the model is the full fish life cycle and the inclusion of life stages of eggs, yolk sac larvae and larvae. In our update we provide movement sub models for these pelagic life stages.

**Spawn-migration:** During the months October–May if SST is below the 9 °C spawning trigger threshold then mature fish move towards offshore spawning grounds.

**Feeding-migration:** When spawning period is over at the end of May each mature fish moves back towards or within its assigned coastal feeding ground.

**Local-movement:** Each juvenile fish moves randomly within coastal patches. Juveniles less than 32 cm (not yet classed as “adolescent”) are further constrained to nursery coastal patches.

**Larval stages drift:** Each egg, yolk-sac larvae and larva move one patch closer to its assigned coastal feeding ground.

**Reproduction:** On the 17th of March mature sea bass calculate their potential fecundity and then the energy required to produce this number of eggs ( $Max_R$ ):

$$Max_R = M_{str} * EG_{pw} * EG_m * (E_f + F_s) \tag{5}$$

where  $M_{str}$  is Structural mass of sea bass (i.e., not including any fat reserves or gonad mass),  $EG_{pw}$  is number of eggs per kg of sea bass (Pickett and Pawson, 1994),  $EG_m$  is the weight of eggs,  $E_f$  is the energy in flesh and  $F_s$  is the cost of synthesising flesh. If there is enough energy to produce maximum potential fecundity, then the energy needed to do this is deducted from energy reserves and gonad mass and realised fecundity are set accordingly. However, if there is not enough energy to reach maximum fecundity then energy reserve is set to whatever is left after subtracting maintenance costs and gonad mass and realised fecundity is set to what is achievable with the limited resources. Once calculated for all mature sea bass, a random sample of 10 mature sea bass super-individuals spawn (introduce one super-individual into the model) which represents as many eggs as determined by total realised fecundity of the whole spawning stock divided by 10. The number of eggs is therefore based on the cumulative available energy reserves. With only 10 individuals spawning the number of super-individuals remains consistent for each cohort and 10 new super-individuals continue to represent the spatial aspect of the fishery (for details see TRACE sections 7, 8.7 and see Table 1 for parameter values).

2.1.3. Model calibration

The model contains 25 parameters, and the values were where possible taken from literature (see TRACE section 5 and TRACE Table 2). Where absolute values of these parameters could not be directly taken from the literature, we used a version of Approximate Bayesian Computation (ABC) called Simulated Annealing ABC (Albert, Künsch and Scheidegger, 2015) as implemented in the Python library ABCpy (Dutta et al., 2017). In all, we estimated 5 parameters using ABC:  $H$ , half saturation constant;  $AM$ , adult natural mortality;  $AE$ , absorbed energy;  $PM$ , pelagic mortality; and  $I$ , importance of density dependence. This method is highly parallelizable, making it an excellent algorithm for use

Table 2

Values for priors, posterior mean and 95% credible intervals for parameters obtained by ABCpy.  $H$ : half saturation constant,  $AM$ : adult natural mortality;  $AE$ : absorbed energy,  $PM$ : pelagic mortality,  $I$ : importance of density dependence. For rationale for choice of priors see TRACE section 9.4.

Parameter	Priors	Posterior mean	95% credible intervals
<b>H</b>	$2.5 \times 10^{-1}, 7.5 \times 10^{-1}$	$4.87 \times 10^{-1}$	$3.04 \times 10^{-1}, 7.26 \times 10^{-1}$
<b>AM</b>	$2.8 \times 10^{-4}, 5.9 \times 10^{-4}$	$4.71 \times 10^{-4}$	$3.43 \times 10^{-4}, 5.87 \times 10^{-4}$
<b>Ae</b>	$0.0, 3 \times 10^{-3}$	$1.64 \times 10^{-3}$	$2.51 \times 10^{-4}, 2.88 \times 10^{-3}$
<b>PM</b>	$4.5 \times 10^{-2}, 1.35 \times 10^{-1}$	$8.01 \times 10^{-2}$	$5.76 \times 10^{-2}, 1.02 \times 10^{-1}$
<b>I</b>	$2.5 \times 10^{+13}, 7.5 \times 10^{+13}$	$5.14 \times 10^{+13}$	$2.72 \times 10^{+13}, 7.39 \times 10^{+13}$

Table 3

Estimated correlation matrix between the parameters shown in Table 2.

-	AM	Ae	PM	I
<b>H</b>	0.19	-0.04	0.06	0.02
<b>AM</b>		-0.04	-0.47	-0.05
<b>Ae</b>			0.35	0.17
<b>PM</b>				0.13

by high-performance computers. ABC began by randomly drawing values of  $H$ ,  $AM$ ,  $AE$ ,  $Pm$  and  $I$  from uniform prior distributions (for full details of priors see TRACE section 9.4) and ran the IBM with these parameter values. Subsequent runs were guided according to how well the outputs of previous runs fitted data as indicated by the sum of the weighted Euclidean distance between the model outputs and data. The data used for parameter calibration was from the sea bass stock assessment model (stock synthesis 3, SS3). These outputs include annual time series of spawning stock biomass [SSB], numbers-at-age, and weight-at-age. SS3 outputs for SSB and numbers at age are estimated annually, however mass at age is simply taken as the stock assessment parameters of the von Bertalanffy model. It is necessary to include mass at age in the calibration to get a realistic population size structure, and in the absence of real data this is the best available guide. The estimated posterior means for all five parameters and 95% credible intervals are shown in Table 2 together with the prior distributions used. The estimated correlation matrix between parameters is shown in Table 3 and the values shown suggest medium to weak correlations between these five model parameters, with a maximum of -0.47 between parameters  $PM$  and  $AM$ .

To quantify the uncertainty in predictions that results from uncertainty in the five calibrated parameters, we ran a posterior predictive check by drawing 111 parameter samples from the inferred approximate posterior distribution and simulating 111 data sets, each using a different parameter sample. From these we obtained posterior predictive inter-quartile ranges, and these are shown in Figs. 3-5 to indicate the uncertainty in predictions.

2.1.4. Sensitivity analysis

The sensitivities of model outputs for SSB and numbers/mass at age are shown in Table 4 as percentage change in output for a 10% decrease/increase in the energy budget model parameters of Table 1. The model remains robust against most parameters with most sensitivities less than 10%. The model was most sensitive to changes in length weight parameter ( $b.g$ ). For the full table of sensitivities of number and mass at age see TRACE section 12.

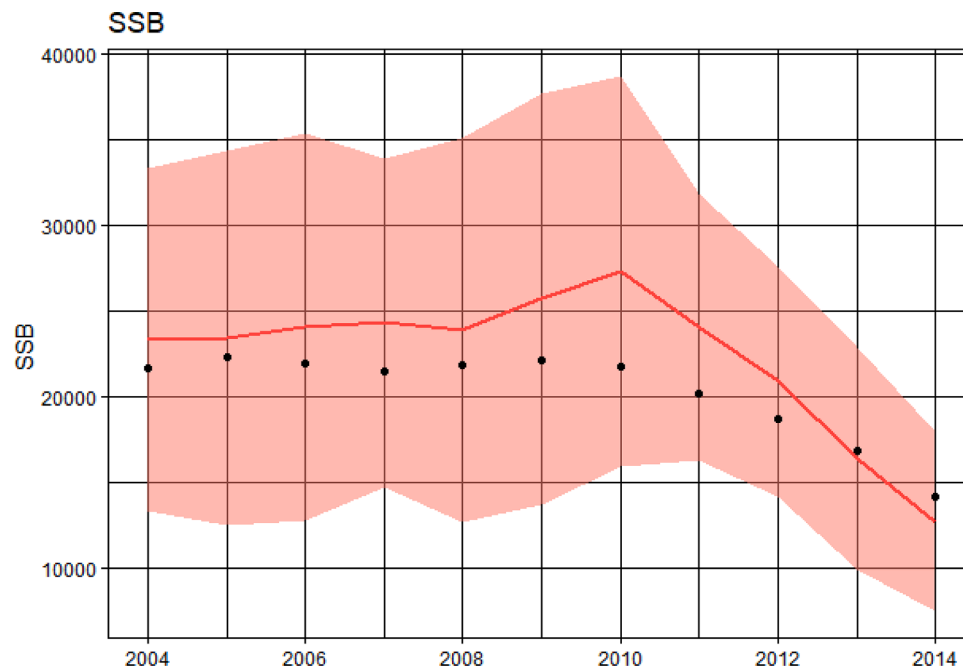


Fig. 3. Model calibration for Spawning Stock Biomass (SSB) for years 2004–2014. Black dots represent the outputs of SS3; solid red line is the median of the IBM posterior predictive distribution; ribbon represents interquartile range.

### 3. Results

To assess the model fits to data, we compare the IBM outputs for SSB and numbers/mass at age with outputs from stock synthesis 3 from 2004 to 2014 (ICES, 2019), as shown in Figs. 3–5. In these figures the black points represent the ‘data’, i.e., outputs from stock synthesis 3, and the solid red lines/dots are IBM outputs using posterior medians. Uncertainty about these outputs is indicated by ribbons representing posterior

predictive inter-quartile ranges.

SSB is the total mass of all fish that are mature (>42 cm). The fit of SSB is shown in Fig. 3. The IBM captures the shape of the data well and follows the decline in SSB from 2010 suggested by the SS3 data. Mass-at-age predictions are assessed by reference to the von Bertalanffy growth curve assumed by SS3 (Fig. 4), which assumes no variation year-to-year. The model slightly overpredicts mass for ages 0 to 4, and underpredicts mass after age 7. The fit of numbers-at-age predictions are shown in

Table 4

Sensitivities of SSB, mean mass at age, and numbers at age, to changes in energy budget model parameters of Table 1. Results are presented as % change in output for a 10% decrease/increase in parameter value relative to values in Table 1 or, for the five fitted parameters, the posterior means shown in Table 2. For mass and numbers at age we show the range of values for brevity, for full table see TRACE section 12 and TRACE Table 6.

Parameter	Value	Output Variable		Mass at age		Numbers at age	
		SSB		Decrease	Increase	Decrease	Increase
linf	84.55	-9.56	0.79	-21.9,0.8	-12.0,25.7	-2.1,7.5	-10.5,3.6
K	0.096699	-1.68	10.52	-20.5,2.7	-4.8,21.5	-2.7,12.3	-2.5,11.6
t0	-0.73	-7.60	-1.53	-16.3,2.0	-14.1,2.7	-1.8,17.1	-2.0,6.6
Ea	0.5	1.71	-0.45	-10.1,4.0	-9.9,2.8	-1.8,10.8	-2.2,2.0
EaS	0.1903656	10.13	-0.67	-10.8,4.7	-10.0,7.6	-2.5,7.7	-1.7,3.2
Cmax	0.54	4.12	6.53	-9.4,7.5	-5.3,6.4	-2.0,13.5	-1.9,10.2
ep	6.02	-1.27	2.18	-9.8,5.6	-10.8,5.1	-1.6,3.7	-3.0,19.4
A0	0.1227808	7.09	-2.12	-7.2,9.9	-6.5,3.1	-1.2,10.1	-2.6,7.9
Ef	7	-11.62	-8.11	-9.3,3.8	-11.6,7.4	-2.3,11.6	-2.3,8.5
El	39.3	4.52	-6.25	-8.3,3.5	-13.4,2.3	-2.4,2.4	-2.5,14.3
Ls	14.7	-10.30	0.55	-17.8,5.5	-8.9,2.6	-2.4,9.3	-2.6,8.1
Fs	3.6	-1.50	0.12	-12.3,2.3	-7.5,3.8	-1.8,14.5	-1.8,11.3
egg_mass	0.00096	5.58	4.29	-16.7,5.9	-8.7,3.4	-1.5,21.8	-3.4,2.0
a_g	$1.23 \times 10^{-5}$	-5.00	10.66	-17.8,-7.2	2.9,16.0	-1.6,6.7	-2.1,20.4
b_g	2.969	-61.27	152.43	-72.9,-45.0	29.8,265.7	-57.5,5.3	-1.2,5.8
eggs_per_bass	375,000	-0.06	-4.45	-11.4,9.4	-22.0,3.9	-1.7,10.5	-2.1,13.9
Gl	0.02485	3.66	-0.78	-7.8,7.7	-11.2,3.9	-28.2,17.6	-2.1,51.8
H	$4.46 \times 10^{-1}$	0.67	6.65	-5.3,6.1	-5.8,7.4	-2.7,9.7	-3.3,11.7
AM	$4.91 \times 10^{-4}$	-0.89	3.49	-8.9,5.0	-6.8,6.4	-0.7,8.9	-3.3,6.8
AE	$1.57 \times 10^{-3}$	1.52	6.78	-17.5,2.7	-8.4,4.7	-3.4,19.0	-1.8,10.6
PM	$8.42 \times 10^{-2}$	1.18	-1.46	-7.4,3.7	-7.5,4.4	-1.3,71.9	-37.1,2.7
I	$5.20 \times 10^{13}$	2.75	5.49	-7.2,4.3	-10.8,4.8	-2.7,2.4	-3.6,5.6

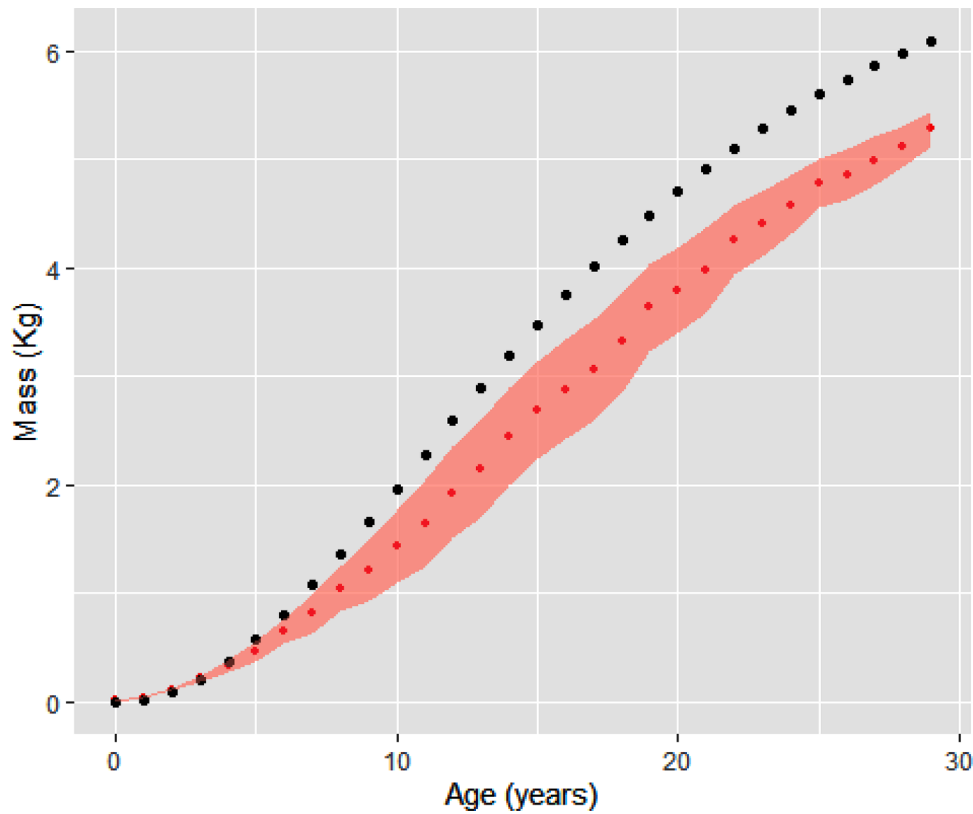


**Fig. 4.** Model calibration for individual average masses (kg) over years 2004–2014 of 30 age classes. Black dots represent the Bertalanffy growth curve used by SS3; red dots are the median of the IBM posterior predictive distribution; ribbon represents interquartile range (which is calculated for each age as the average of the yearly interquartile ranges). For model fits of each of the 30 age classes for years 2004–2014 see TRACE section 11.

**Fig. 5.** Model fits to the SS3 data are good for ages 5 and above, and reasonably good for all ages. In addition to the calibration plots (Figs, 3, 4 and 5) we show some spatial model outputs in Fig. 6. These show the spatial intra-annual spatial distribution of sea bass biomass; note there is also interannual variation which can be seen in the TRACE figure 19.

**4. Discussion**

Here we have presented a spatially explicit individual based model of the northern stock of sea bass which has been calibrated and assessed for

goodness of fit against stock synthesis 3 outputs of SSB and the numbers and individual masses of 30 age classes. The model builds on Walker et al. (2020), but our addition of individual energy budgets driven by phytoplankton density provides a mechanistic link between environmental drivers and fish populations. We also present spatial outputs of biomass distribution to demonstrate how the energy budget creates a mechanistic link between changes in environmental drivers and predictions of temporal and spatial distribution of sea bass. The energy budget approach follows established methods (Boyd, Walker, et al., 2020; Mintram et al., 2020; Watson et al., 2020). Our model is intended

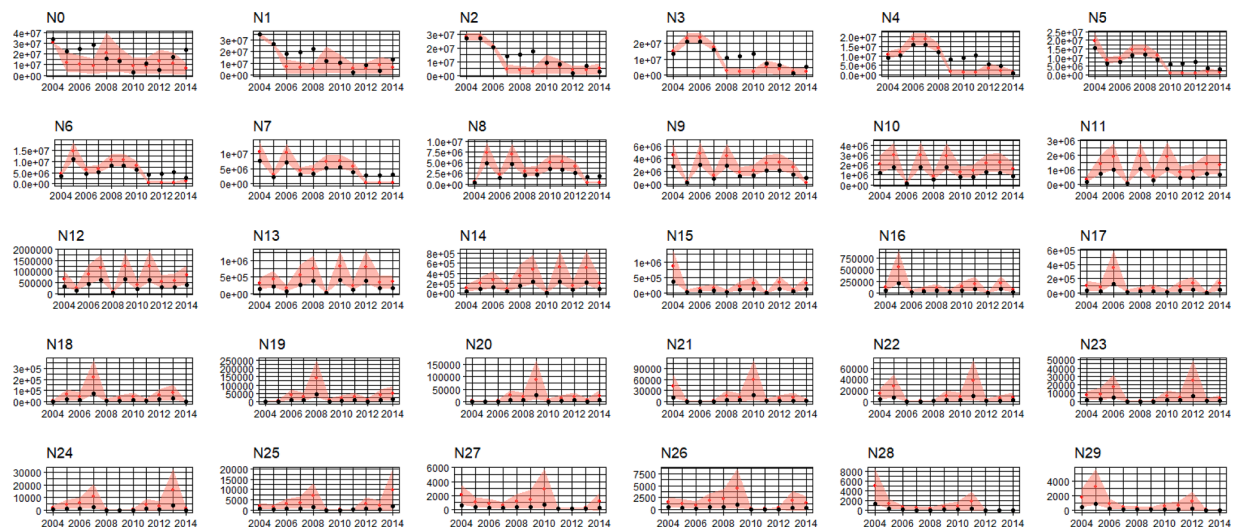


**Fig. 5.** Model calibration for numbers in 30 age classes for years 2004–2014. N0 = number at age 0, N1 = number at age 1, etc. Black dots represent the outputs of SS3; red dots are the median of the IBM posterior predictive distribution; ribbon represents interquartile range.

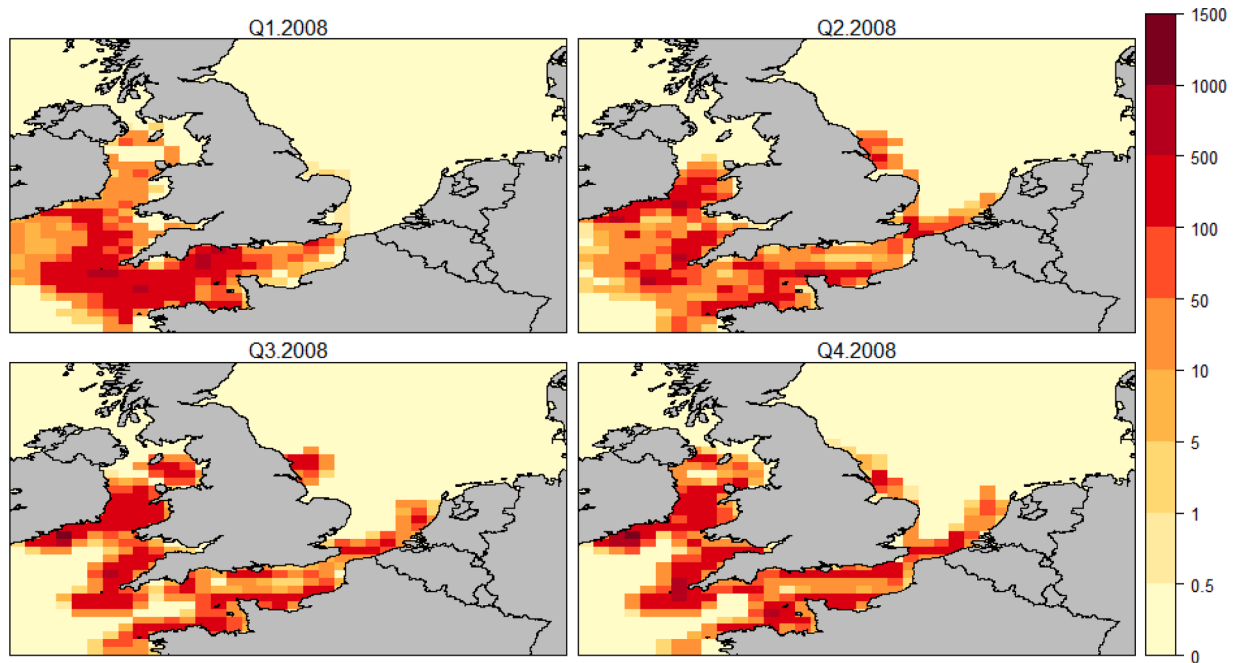


**Fig. 6.** Mean daily biomass (tonnes) distribution per quarter for the year 2008. Q1 = 1st January – 31st March, Q2 = 1st April – 30th June, Q3 = 1st July – 30th September, Q4 = 1st October – 31st December. Note that no data are currently available with which to compare these results.

for use by fisheries managers to complement, not replace, current stock assessment approaches using SS3.

A key assumption in our model is that local food density available to sea bass can be represented by observed phytoplankton density. Sea bass are generalist predators, and their diet is opportunistic, so it is difficult to predict what they will be eating at any particular time (Pickett and Pawson, 1994). Their food choices could in principle be derived from a model of local ecosystems, but this would require many unobservable parameters (i.e., what, when and where sea bass are eating and the associated uncertainty). We therefore chose instead to make use of remote sensing data of phytoplankton blooms which constitute the base of the marine food web. There are several problems in attempting to estimate how much of the energy present in phytoplankton is feasibly available to sea bass. We reason that areas of high phytoplankton density are likely favourable to all trophic levels; that is, they will correlate with high densities of species that directly consume phytoplankton and consequently will be attractive to species that prey upon these secondary consumers and a continuation of this pattern up the food chain. Further, many species in the marine environment (including much of sea bass prey) are highly mobile and may move around seeking energy in the form of their preferred prey. On the other hand there is likely a delay (which we term *trophic delay*) in time from a large amount of energy being present in the form of phytoplankton till it is available to sea bass as a range of prey (because prey species increase in biomass through individual growth or reproduction). In this model we bypass these complexities by using a single parameter *absorbed energy* to indicate how much of the phytoplankton ends up in the fish. Our approach can be considered justified by the good fits to the data seen in Figs. 3, 4 and 5.

Methods of calibrating and evaluating complex models have advanced considerably in recent years. Here we used Simulated Annealing ABC (SABC [Albert, Künsch and Scheidegger, 2015]) to calibrate five model parameters (adult and pelagic mortality rates, absorbed energy and two density dependences) that would otherwise be extremely difficult to estimate. SABC is much faster and more accurate than rejection ABC methods (Dutta et al., 2017) which have previously been used to calibrate similar IBMs (e.g., Boulton et al., 2018; Boyd, Walker, et al., 2020; van der Vaart et al., 2015).

The model outputs we have presented give insight into how different

aspects of the model are working. Spawning stock biomass (SSB, Fig. 3) is the size of the mature stock, which is the basis for setting legislative targets to manage the stock. We see good fits for SSB across the simulation period. We also see good fits to body weights-at-age (Fig. 4) which suggests that both the numbers and sizes of the individuals are reasonable. The numbers and masses in each age class are discussed below.

The numbers in each age class are shown in Fig. 5. Assessing numbers at age rather than total abundance is necessary to avoid the more numerous younger fish dominating the model fits. Overall, the dynamic model age structure shown in Fig. 5 is a good fit against the SS3 data, although some of the goodness of fit may stem from what happens in the spin up period. Cohorts born in the spin up period are read in from ICES numbers at age data, and their numbers thereafter are only affected by two model parameters, natural mortality (*AM*) and fishing mortality.

The *N0* panel shown in Fig. 5 represents the number of fish that are age 0 and no longer in the pelagic stage (defined in our model as an individual with age < 1 and Length > 1.4 cm [Beraud et al., 2018]). Predicted *N0* fits SS3 data well in some years but in others there are significant discrepancies. Discrepancies almost certainly arise from lack of realism in our model, —predicting recruitment is famously difficult—, but may also arise from errors in the SS3 ‘data’. The SS3 estimates of the *N0* are outputs of a population-dynamics model described in the Introduction, and subject to some uncertainty. So the discrepancies between our predictions and the SS3 data do not necessarily mean our predictions are wrong. *N0* (i.e., the number of *N0* individuals) in our model is an emergent property driven by the number of mature fish and their spawning success, which depends on the condition of the parents (Mcbride et al., 2015), and early survival. Larger fish with higher fat reserves can produce more eggs (i.e., have higher potential fecundity) than smaller fish, so the more mature fish there are in the simulation, the greater their collective realised fecundity. If the mature fish have had access to abundant energy, there is more left to produce eggs after the necessary allocation to maintenance and growth. It is important to note that the model does not cover quality of eggs though there is some evidence that fish that have had access to better nutrition may also be able to produce higher quality eggs, which may increase larval survival and stock recruitment (Cerdá et al., 1994; Chatzifotis et al., 2011). In the model presented the amount of energy to produce

eggs is also influenced by temperature, since individuals in warmer sea temperatures may ingest more energy, grow faster and have higher levels of reserves from which to produce eggs. The other major contributor to the N0 output is pelagic natural mortality rate. The daily pelagic mortality rate  $8.01 \times 10^{-2}$  is far greater than that of the adult mortality parameter in our model  $4.71 \times 10^{-4}$ , so there is a substantial payoff to growing faster to escape the pelagic phase earlier. In this way the number of larvae that make it through to be juvenile fish (i.e., classified as N0) is dependant on their growth rate, which in turn depends on food availability, temperature, and the density of competitors.

The masses of the individuals in each age class are presented in Fig. 4. Although the models provide fairly good fits for younger fish, the masses of older fish are underpredicted. Discrepancies between our predictions and the SS3 data do not necessarily mean our predictions are wrong, because the SS3 'data' are simply outputs of a fitted von Bertalanffy growth curve (ICES, 2021). Discrepancies may also arise as a result of the spin-up process. During spin up we read in the numbers at age 0 estimates from SS3 as is done in the spawning sub models of Walker et al. (2020), but afterwards spawning is determined by the fishes' energy budgets, and the two methods differ in when spawning takes place. The result is that the IBM age 0 cohort consists of older and larger fish than in the SS3 data. As the cohort ages it continues heavier for a few years, and this may explain the overpredictions of mass for M0 – M4 in the first few years of the simulations (see Figure 17 in TRACE section 11). The underpredictions of masses of older fish are harder to explain but may result from some lack of realism in our representation of energy budgets. In our model an individual's mass depends on its history of ingesting energy, and this in turn depends on the energy available in the environment, competition from other fish and sea surface temperature and this is what the AE and I parameters hoped to capture. In excess of structural mass individuals have the potential to put on weight as fat reserves. High reserves result from abundant energy, high SST and/or low competition, and eventually allow mature individuals to spawn. These processes result in fluctuations in fat reserves that the SS3 assessment does not capture.

There are many potential fisheries management applications for the IBM we present here. The original model published by Walker et al., 2020 was designed to complement the SS3 stock assessment and to test spatial management scenarios, and the updated model here still retains that utility (though note movement sub model limitations discussed below). We demonstrate some of the spatial and temporal inter (TRACE Figure 19) and intra annual variation utility in Figure 6 where results show predictions of variation in the distribution of sea bass. Our energy budget additions and the subsequent emergent population dynamics that are driven by the environmental drivers make the model a good tool to study a range of climate impacts on the stock. Using different climate projections the energy budget could capture the effect of temperature on life processes of ingestion, metabolic rate, growth and sea bass recruitment (known to be heavily influenced by temperature [Pawson, Pickett and Smith, 2005]) and the subsequent impacts of the stock could be analysed. Another advantage of the full fish life cycle and closed energy budget additions is that changes in condition or number of the spawning stock will have consequences on the following year's recruitment. This closed loop facilitates testing of a range of existing and new management measures for recreational and commercial fishing (e.g., spatial, and temporal closures, changes to total allowable catch/minimum landing size, bag limits etc.).

The model is built in a modular fashion making additions or changes to further the model utility achievable. One promising line of work is to add other dynamic maps of anthropogenic stressors to the model environment. For example, the addition of a soundscape map to which the individuals would suffer sublethal effects through reduced ingestion and the knock-on effects through the energy budget (Watson et al., 2020) would give rise to emergent population effects of anthropogenic noise (a similar approach was done for porpoise in a study by Nabe-Nielsen et al., 2014). In addition, there is scope to update fishing pressure which is

currently read in from ICES data to a more mechanistic sub model. Sea bass are mostly targeted by the under 10 m fleet in the UK (Williams et al., 2018) and the small vessels are often most vulnerable to bad weather (Sainsbury et al., 2018; Young et al., 2019). An updated fishing pressure sub model that responded mechanistically to environmental and socio-economic pressures would further develop the model utility to fisheries management (e.g., [Jules Dreyfus-León, 1999; Millischer and Gascuel, 2006; Bastardie et al., 2010; Bailey et al., 2019; Lindkvist et al., 2020]).

We believe that the IBM we present here is a useful tool in its current form, however there are some caveats and further opportunities for improvement. Firstly, a general critique of individual/agent based models is the large amount of data that they require for model parameterisation, calibration, and validation (Johnston et al., 2019). To calibrate and assess the fits of the model, we use outputs from the sea bass SS3 assessment model. The SS3 model takes all the available data from surveys and literature to assess the state of the stock (ICES, 2021) and outputs modelled 'data', so we are fitting the IBM model outputs to another model's outputs. This is suboptimal but in the absence of the extensive long-term field data on individuals, outputs from SS3 remain the best calibration option and the limited availability of calibration data may also explain why the credible intervals remain wide for the five parameters fitted with ABC (Table 2). Further detailed spatial distribution data would also be required to truly validate the spatial and temporal explicit predictions by the model (shown in Fig. 6) Another limitation is the movement sub model which remains unchanged from Walker et al., 2020. Walker et al., 2020 outline how modern tagging methods (Quayle et al., 2009; O'Neill et al., 2018; de Pontual et al., 2019) could provide data on which a mechanistic movement sub model could be built and added to further the spatial utility of the model. To conclude we hope that fisheries managers may find the spatial, mechanistic, and emergent merits of this IBM a useful complementary tool to SS3 with scope for further development to aid the sustainable management of northern sea bass stock.

#### Declaration of competing interest

The authors declare that they have no known competing financial interests or personal relationships that could have appeared to influence the work reported in this paper.

#### Acknowledgments

Authors were supported as follows; JW was funded by a NERC PhD studentship [grant number NE/L002566/1] with CASE sponsorship from CEFAS, GV and RE are funded by NERC (NE/T00973X/1) and RD is funded by EPSRC (grant nos. EP/V025899/1, EP/T017112/1) and NERC (grant no. NE/T00973X/1), RMS was part funded by NERC (NE/T004010/1). The authors also thank the Scientific Computing Research Technology Platform (SCRTP) at the University of Warwick for the computing resource.

#### Supplementary materials

Supplementary material associated with this article can be found, in the online version, at doi:10.1016/j.ecolmodel.2022.109878.

#### References

- Albert, C., Künsch, H.R., Scheidegger, A., 2015. 'A simulated annealing approach to approximate Bayes computations'. In: Statistics and Computing, 25. Kluwer Academic Publishers, pp. 1217–1232. <https://doi.org/10.1007/s11222-014-9507-8>.
- Annis, E.R., et al., 2011. Calibration of a bioenergetics model linking primary production to Atlantic menhaden *Brevoortia tyrannus* growth in Chesapeake Bay. *Marine Ecol. Progr. Ser.* 437, 253–267. <https://doi.org/10.3354/meps09254>.
- Augusiak, J., Van den Brink, P.J., Grimm, V., 2014. Merging validation and evaluation of ecological models to "evaluation": a review of terminology and a practical

- approach. *Ecol. Modell.* Elsevier B.V. 280, 117–128. <https://doi.org/10.1016/j.ecolmodel.2013.11.009>.
- Bailey, R.M., et al., 2019. A computational approach to managing coupled human–environmental systems: the POSEIDON model of ocean fisheries. In: *Sustainability Science*, 14. Springer, Tokyo, pp. 259–275. <https://doi.org/10.1007/s11625-018-0579-9>.
- Bastardie, F., et al., 2010. Effects of fishing effort allocation scenarios on energy efficiency and profitability: an individual-based model applied to Danish fisheries. In: *Fisheries Research*, 106. Elsevier, pp. 501–516. <https://doi.org/10.1016/j.fishres.2010.09.025>.
- Edited by Beraud, C., et al., 2018. The influence of oceanographic conditions and larval behaviour on settlement success—the European sea bass *Dicentrarchus labrax* (L.). In: Kaplan, D. (Ed.), *ICES Journal of Marine Science*, 75, pp. 455–470. <https://doi.org/10.1093/icesjms/fsx195>. Edited by.
- Boult, V.L., et al., 2018. Individual-based modelling of elephant population dynamics using remote sensing to estimate food availability. *Ecol. Modell.* 387, 187–195. <https://doi.org/10.1016/j.ecolmodel.2018.09.010>.
- Boult, V.L., et al., 2019. Human-driven habitat conversion is a more immediate threat to Amboseli elephants than climate change. In: *Conservation Science and Practice*, 1. Wiley, p. e87. <https://doi.org/10.1111/csp2.87>.
- Boyd, R., Thorpe, R., et al., 2020. Potential consequences of climate and management scenarios for the Northeast Atlantic mackerel fishery. In: *Frontiers in Marine Science*, 7. Frontiers, p. 639. <https://doi.org/10.3389/fmars.2020.00639>.
- Boyd, R., Walker, N., et al., 2020. SEASIM-NEAM: a spatially-explicit agent-based SIMulator of North East Atlantic Mackerel population dynamics. In: *MethodsX*, 7. Elsevier B.V., 101044 <https://doi.org/10.1016/j.mex.2020.101044>
- Bueno-Pardo, J., et al., 2020. Integration of bioenergetics in an individual-based model to hindcast anchovy dynamics in the Bay of Biscay. *ICES J. Mar. Sci.* <https://doi.org/10.1093/icesjms/fsz239>.
- Cerdá, J., et al., 1994. Influence of nutritional composition of diet on sea bass, *Dicentrarchus labrax* L., reproductive performance and egg and larval quality. In: *Aquaculture*, 128. Elsevier, pp. 345–361. [https://doi.org/10.1016/0044-8486\(94\)90322-0](https://doi.org/10.1016/0044-8486(94)90322-0).
- Chatzifotis, S., et al., 2011. Effect of starvation and re-feeding on reproductive indices, body weight, plasma metabolites and oxidative enzymes of sea bass (*Dicentrarchus labrax*). *Aquaculture* 316 (1–4), 53–59. <https://doi.org/10.1016/j.aquaculture.2011.02.044>.
- Claireaux, G., 2006. Effect of temperature on maximum swimming speed and cost of transport in juvenile European sea bass (*Dicentrarchus labrax*). In: *Journal of Experimental Biology*, 209. The Company of Biologists Ltd, pp. 3420–3428. <https://doi.org/10.1242/jeb.02346>.
- DeAngelis, D.L., Grimm, V., 2014. Individual-based models in ecology after four decades. *Fl1000Prime Rep.* 6 <https://doi.org/10.12703/P6-39>.
- Dutta, R., et al., 2017. ABCpy: A user-friendly, extensible, and parallel library for approximate Bayesian computation. In: *PASC 2017 - Proceedings of the Platform for Advanced Scientific Computing Conference*. Association for Computing Machinery, Inc. <https://doi.org/10.1145/3093172.3093233>.
- GOV.UK (2020) *Bass fishing guidance 2020 - GOV.UK*. Available at: <https://www.gov.uk/government/publications/bass-industry-guidance-2020/bass-fishing-guidance-2020> (Accessed: 18 June 2020).
- Grimm, V. et al. (2006) 'A standard protocol for describing individual-based and agent-based models'. doi: 10.1016/j.ecolmodel.2006.04.023.
- Grimm, V., et al., 2010. The ODD protocol: a review and first update. *Ecol. Modell.* 221 (23), 2760–2768. <https://doi.org/10.1016/j.ecolmodel.2010.08.019>.
- Grimm, V., et al., 2014. Towards better modelling and decision support: Documenting model development, testing, and analysis using TRACE. In: *Ecological Modelling*, 280. Elsevier B.V., pp. 129–139. <https://doi.org/10.1016/j.ecolmodel.2014.01.018>
- Grimm, V., et al., 2020. The ODD protocol for describing agent-based and other simulation models: a second update to improve clarity, replication, and structural realism. *J. Artif. Soc. Soc. Simul.* 23 (2) <https://doi.org/10.18564/jasss.4259>.
- Heinänen, S., et al., 2018. Integrated modelling of Atlantic mackerel distribution patterns and movements: a template for dynamic impact assessments. In: *Ecological Modelling*, 387. Elsevier B.V., pp. 118–133. <https://doi.org/10.1016/j.ecolmodel.2018.08.010>
- ICES, 2012. Report of the Inter-Benchmark Protocol on New Species (Turbot and Sea bass). In: *ICES CM 2012/ACOM*, 45. Copenhagen (October).
- ICES, 2019. ICES Advice: Sea bass (*Dicentrarchus labrax*) in Divisions 4.b–c, 7.a, and 7.d–h (central and southern North Sea, Irish Sea, English Channel, Bristol Channel, and Celtic Sea). Rep. ICES Advisory Committee. <https://doi.org/10.17895/ices.advice.4779>.
- ICES (2021) *Working group for the Celtic seas ecoregion (WGCE)*. doi: 10.17895/ices.pub.5978.
- Jennings, S., Jennings, S., Pawson, M.G., 1992. The origin and recruitment of bass, *Dicentrarchus labrax*, larvae to nursery areas. *J. Mar. Biol. Assoc. UK* 72 (1), 199–212. <https://doi.org/10.1017/S0025315400048888>.
- Johnston, A.S.A., et al., 2019. Predicting population responses to environmental change from individual-level mechanisms: towards a standardized mechanistic approach. In: *Proceedings of the Royal Society B: Biological Sciences*, 286. Royal Society Publishing, 20191916. <https://doi.org/10.1098/rspb.2019.1916>.
- Jourdan-Pineau, H., et al., 2010. An investigation of metabolic prioritization in the European Sea Bass, *Dicentrarchus labrax*. *Physiol. Biochem. Zool.* 83 (1), 68–77. <https://doi.org/10.1086/648485>.
- Jules Dreyfus-León, M., 1999. Individual-based modelling of fishermen search behaviour with neural networks and reinforcement learning. *Ecol. Modell.* 120 (2–3), 287–297. [https://doi.org/10.1016/S0304-3800\(99\)00109-X](https://doi.org/10.1016/S0304-3800(99)00109-X).
- Kelley, D.F., 1988. The importance of estuaries for sea-bass, *Dicentrarchus labrax* (L.). *J. Fish Biol.* 33 (sa), 25–33. <https://doi.org/10.1111/j.1095-8649.1988.tb05555.x>.
- Lanari, D., D'Agaro, E., Ballestrazzi, R., 2002. Growth parameters in European sea bass (*Dicentrarchus labrax* L.): effects of live weight and water temperature. *Italian J. Anim. Sci.* 1 (3), 181–185. <https://doi.org/10.4081/ijas.2002.181>.
- Lindkvist, E., et al., 2020. Navigating complexities: agent-based modeling to support research, governance, and management in small-scale fisheries. *Frontiers in Marine Science*. Frontiers Media S.A., p. 733. <https://doi.org/10.3389/fmars.2019.00733>
- Luna-Acosta, A., et al., 2011. Physiological response in different strains of sea bass (*Dicentrarchus labrax*): swimming and aerobic metabolic capacities. *Aquaculture* 317 (1–4), 162–167. <https://doi.org/10.1016/j.aquaculture.2011.03.004>.
- Mcbride, R.S., et al., 2015. Energy acquisition and allocation to egg production in relation to fish reproductive strategies. *Fish. Fisher.* <https://doi.org/10.1111/faf.12043>.
- Method, R.D., Wetzel, C.R., 2013. Stock synthesis: A biological and statistical framework for fish stock assessment and fishery management. In: *Fisheries Research*, 142. Elsevier, pp. 86–99. <https://doi.org/10.1016/j.fishres.2012.10.012>.
- Millischer, L., Gascuel, D., 2006. Information transfer, behavior of vessels and fishing efficiency: an individual-based simulation approach. *Aquatic Living Resour.* 19 (1), 1–13. <https://doi.org/10.1051/alr:2006001>.
- Mintram, K.S., et al., 2020. Applying a mechanistic model to predict interacting effects of chemical exposure and food availability on fish populations. *Aquatic Toxicology*. Elsevier B.V., p. 224. <https://doi.org/10.1016/j.aquatox.2020.105483>
- Nabe-Nielsen, J., et al., 2014. Effects of noise and by-catch on a Danish harbour porpoise population. In: *Ecological Modelling*, 272. Elsevier, pp. 242–251. <https://doi.org/10.1016/j.ecolmodel.2013.09.025>.
- O'Neill, R., et al., 2018. The novel use of pop-off satellite tags (PSATs) to investigate the migratory behaviour of European sea bass *Dicentrarchus labrax*. In: *Journal of Fish Biology*, 92. Blackwell Publishing Ltd, pp. 1404–1421. <https://doi.org/10.1111/jfb.13594>.
- Pawson, M.G., Pickett, G.D., Smith, M.T., 2005. 'The role of technical measures in the recovery of the UK sea bass (*Dicentrarchus labrax*) fishery 1980–2002'. *Fish. Res.* 76 (1), 91–105. <https://doi.org/10.1016/j.fishres.2005.06.006>.
- Peixoto, M.J., et al., 2016. Diets supplemented with seaweed affect metabolic rate, innate immune, and antioxidant responses, but not individual growth rate in European seabass (*Dicentrarchus labrax*). *J. Appl. Phycol.* 28 (3), 2061–2071. <https://doi.org/10.1007/s10811-015-0736-9>.
- Peters, R.H., 1986. *The Ecological Implications of Body Size, The Ecological Implications of Body Size*. Cambridge University Press. <https://doi.org/10.1017/cb09780511608551>.
- Pickett, G.D., Pawson, M.G., 1994. Sea bass: biology, exploitation and conservation. In: *Sea Bass: Biology, Exploitation and Conservation*, 124. Chapman & Hall; Fish and Fisheries Series, 12, pp. 643–644. <https://doi.org/10.1577/1548-8659-124.4.643>.
- Politikos, D.V., Huret, M., Petitgas, P., 2015. A coupled movement and bioenergetics model to explore the spawning migration of anchovy in the Bay of Biscay. *Ecol. Modell.* 313, 212–222. <https://doi.org/10.1016/j.ecolmodel.2015.06.036>.
- Edited by de Pontual, H., et al., 2019. New insights into behavioural ecology of European seabass off the West Coast of France: implications at local and population scales. In: Grabowski, J. (Ed.), *ICES Journal of Marine Science*, 76. Oxford University Press, pp. 501–515. <https://doi.org/10.1093/icesjms/fsy086>. Edited by.
- Quayle, V.A. et al. (2009) 'Observations of the Behaviour of European Sea Bass (*Dicentrarchus labrax*) in the North Sea', in, pp. 103–119. doi: 10.1007/978-1-4020-9640-2-7.
- Regner, S., Dulčić, J., 1994. Growth of sea bass, *Dicentrarchus labrax*, larval and juvenile stages and their otoliths under quasi-steady temperature conditions. In: *Marine Biology*, 119. Springer-Verlag, pp. 169–177. <https://doi.org/10.1007/BF00349553>.
- Sainsbury, N.C., et al., 2018. Changing storminess and global capture fisheries. *Nature Climate Change* 8 (8), 655–659. <https://doi.org/10.1038/s41558-018-0206-x>.
- Scheffer, M., et al., 1995. Super-individuals a simple solution for modelling large populations on an individual basis. *Ecol. Modell.* 80 (2–3), 161–170. [https://doi.org/10.1016/0304-3800\(94\)00055-M](https://doi.org/10.1016/0304-3800(94)00055-M).
- Schmidt-Nielsen, K., 2013. *Animal Physiology: Adaption and Environment*, 5th edn. Cambridge University Press.
- Scholke, A., et al., 2010. Ecological models supporting environmental decision making: a strategy for the future. *Trend. Ecol. Evolut.* 479–486. <https://doi.org/10.1016/j.tree.2010.05.001>.
- Sibly, R.M. et al. (2013) 'Representing the acquisition and use of energy by individuals in agent-based models of animal populations', *Methods in Ecology and Evolution*. Edited by D. Murrell, 4(2), pp. 151–161. doi: 10.1111/2041-210x.12002.
- Sibly, R.M., Calow, P., 1986. *Physiological Ecology of Animals: an Evolutionary Approach*. Blackwell.
- Thompson, B.M., Harrop, R.T., 1987. The distribution and abundance of bass (*Dicentrarchus labrax*) eggs and larvae in the English Channel and Southern North Sea. *J. Mar. Biol. Assoc. UK* 67 (2), 263–274. <https://doi.org/10.1017/S0025315400026588>.
- van der Vaart, E., et al., 2015. Calibration and evaluation of individual-based models using approximate Bayesian computation. In: *Ecological Modelling*, 312. Elsevier, pp. 182–190. <https://doi.org/10.1016/j.ecolmodel.2015.05.020>.
- Walker, N.D., et al., 2020. A spatially explicit individual-based model to support management of commercial and recreational fisheries for European sea bass *Dicentrarchus labrax*. In: *Ecological Modelling*, 431. Elsevier B.V., 109179 <https://doi.org/10.1016/j.ecolmodel.2020.109179>
- Watkins, K.S., Rose, K.A., 2017. Simulating individual-based movement in dynamic environments. In: *Ecological Modelling*, 356. Elsevier B.V., pp. 59–72. <https://doi.org/10.1016/j.ecolmodel.2017.03.025>

- Watson, J., et al., 2020. Assessing the sublethal impacts of anthropogenic stressors on fish: an energy-budget approach. In: *Fish and Fisheries*, 21. John Wiley & Sons, Ltd, pp. 1034–1045. <https://doi.org/10.1111/faf.12487>.
- Wilensky, U., 1999. 'NetLogo'. Center for Connected Learning and ComputerBased Modeling Northwestern University Evanston IL, Evanston, IL.
- Williams, C., et al., 2018. 'Who gets to fish for sea bass? Using social, economic, and environmental criteria to determine access to the English sea bass fishery. In: *Marine Policy*, 95. Elsevier Ltd, pp. 199–208. <https://doi.org/10.1016/j.marpol.2018.02.011>.
- Edited by Young, T., et al., 2019. Adaptation strategies of coastal fishing communities as species shift poleward. In: Makino, M. (Ed.), *ICES Journal of Marine Science*, 76. Oxford University Press, pp. 93–103. <https://doi.org/10.1093/icesjms/fsy140>. Edited by.
- Zupa, W., et al., 2015. Modelling swimming activities and energetic costs in European sea bass (*Dicentrarchus labrax* L., 1758) during critical swimming tests. *Mar. Freshwater Behav. Physiol.* 48 (5), 341–357. <https://doi.org/10.1080/10236244.2015.1073456>.